Inorganic Chemistry

ARTICLE

pubs.acs.org/IC

Anion Binding in the C_{3v}-Symmetric Cavity of a Protonated Tripodal Amine Receptor: Potentiometric and Single Crystal X-ray Studies

Purnandhu Bose, I. Ravikumar, and Pradyut Ghosh*

Department of Inorganic Chemistry, Indian Association for the Cultivation of Science, 2A & 2B Raja S. C. Mullick Road, Kolkata 700 032, India

Supporting Information

ABSTRACT:

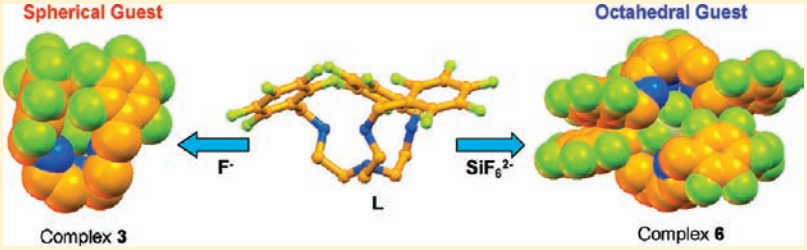

Tris(2-aminoethyl)amine (tren) based pentafluorophenyl-substituted tripodal **L**, tris[[(2,3,4,5,6-pentafluorobenzyl)amino]ethyl]-amine receptor is synthesized in good yield and characterized by single crystal X-ray diffraction analysis. Detailed structural aspects of binding of different anionic guests toward **L** in its triprotonated form are examined thoroughly. Crystallographic results show binding of fluoride in the C_{3v}-symmetric cavity of $[H_3\mathbf{L}]^{3+}$ where spherical anion fluoride is in tricoordinated geometry via $(N-H)^+\cdots F$ interaction in the complex $[H_3\mathbf{L}(F)]\cdot[F]_2\cdot 2H_2O$, (**3**). In the case of complexes $[H_3\mathbf{L}(OTs)]\cdot[OTs]_2$, (**4**) and $[H_3\mathbf{L}(OTs)]\cdot[NO_3]\cdot[OTs]$, (**5**), tetrahedral *p*-toluenesulphonate ion is engulfed in the cavity of $[H_3\mathbf{L}]^{3+}$ via $(N-H)^+\cdots O$ interactions. Interestingly, complex $[(H_3\mathbf{L})_2(SiF_6)]\cdot[BF_4]_4\cdot CH_3OH\cdot H_2O$, (**6**) shows encapsulation of octahedral hexafluorosilicate in the dimeric capsular assembly of two $[H_3\mathbf{L}]^{3+}$ units, via a number of $(N-H)^+\cdots F$ interactions. The kinetic parameters of **L** upon binding with different anions are evaluated using a potentiometric study in solution state. The potentiometric titration experiments in a polar protic methanol/water (1:1 v/v) binary solvent system show high affinity of the receptor toward more basic fluoride and acetate anions, with a lesser affinity for other inorganic anions (e.g., chloride, bromide, nitrate, sulfate, dihydrogenphosphate, and *p*-toluenesulphonate).

INTRODUCTION

Recognition of anions has a remarkable impact because of its biological and environmental importance.[1] The development of efficient receptors capable of binding a specific anion is challenging in the area of anion sensing, extraction, and separation technology.[2−12] Protonated amines and quaternary ammonium functions incorporated into a suitable ligand topology make attractive receptors for anions mainly because of a balanced combinations of both the electrostatic and the hydrogen-bonding interactions with the anionic guest. The tris(2-aminoethyl)amine (tren) is one of the much used scaffolds for anion coordination studies.[13−33] The binding ability of tren-based acyclic tripodal receptors toward anions varies with the attached functionality to the tren (N_4) unit, since functional groups have the tendency to modify the hydrogen bonding capability, as well as the conformation of the receptor.[25] One of the important criteria for recognition of an anionic guest is to create a suitable cavity/cleft in the receptor designing to overcome the high solvation energy of anions. Bowman-James et al. have reported a tren based phenyl substituted triprotonated ligand which can bind bromide in the cleft formed by two extended arms with a quasi-planar C_{2v} symmetry.[26] On the other hand, anion recognition in C_{3v} symmetric cavity by tren-based systems are mostly found in polyammonium bicyclic cages.[34−38] Interestingly, tren has also shown the formation of a C_{3v} symmetric tripodal cavity in cases of tren-hydrochloride, tren-nitrate, and tren-tosylate salts where anions are located outside the C_{3v}-symmetric cavity.[39,40] At this juncture, we came up with an idea to attach an electron deficient pentafluorophenyl substituent to construct a tren based tripodal amine receptor for encapsulation of chloride and bromide in the C_{3v}-symmetric cavity of $[H_3\mathbf{L}]^{3+}$, complexes **1** and **2**, respectively (Chart 1).[27] Herein, we describe a detailed anion binding study of $[H_3\mathbf{L}]^{3+}$ in the solid as well as in solution states. In particular, we structurally demonstrate the encapsulation of spherical fluoride (**3**) and tetrahedral *p*-toluenesulphonate (**4** and **5**) in the cavity of $[H_3\mathbf{L}]^{3+}$. Interestingly, we also show a single crystal X-ray structural evidence of a dimeric capsular assembly of the $[H_3\mathbf{L}]^{3+}$ receptor with an octahedral hexafluorosilicate anion (**6**) (Chart 1). A detailed potentiometric

Received: May 30, 2011
Published: September 26, 2011

Chart 1. Tripodal Receptor L, Triprotonated Complexes of L with Halides (1−3); *p*-Toluenesulphonate Complexes of L, (4−5); and Hexafluorosilicate Assisted Capsular Assembly, 6

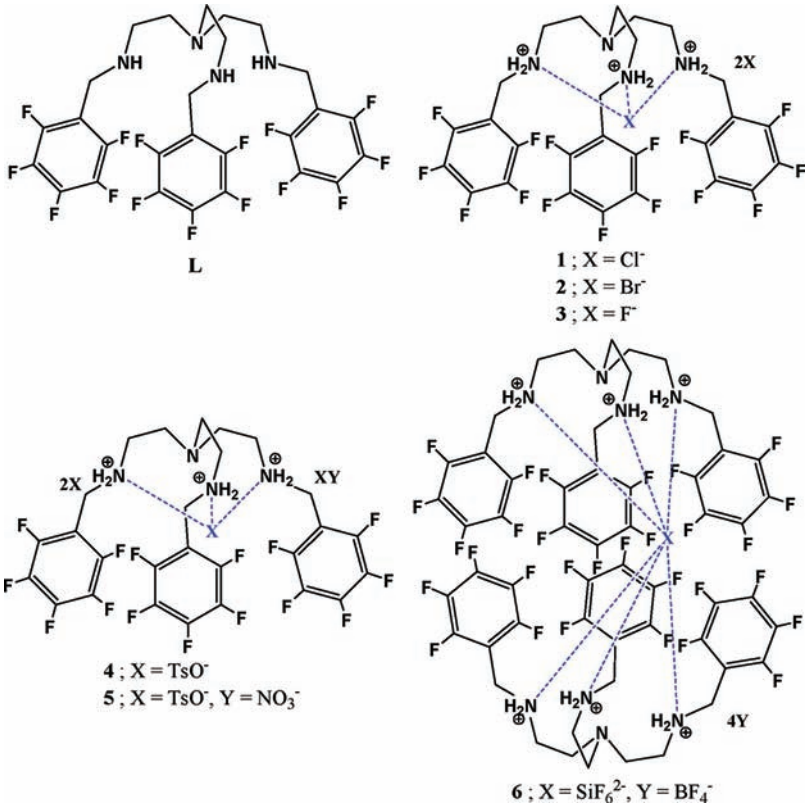

study is also carried out to determine the kinetic parameters upon anion binding by $[H_3L]^{3+}$ in the solution state.

EXPERIMENTAL SECTION

Materials and Methods. Tris(2-aminoethyl)amine (tren), 2,3,4,5,6-pentafluorobenzaldehyde, sodium tosylate, and *n*-tetrabutylammonium salts of fluoride, chloride, bromide, iodide, acetate, nitrate, hydrogensulphate and dihydrogenphosphate were purchased from Sigma-Aldrich and used without further purification. Sodium borohydride, chloroform, methanol, carbonate free sodium hydroxide, sodium nitrate, and *p*-toluenesulphonic acid monohydrate were procured from SD-Fine Chemicals Limited, India. ^{1}H NMR and ^{13}C NMR spectra were obtained at 300 and 75 MHz on a Bruker DPX-300 FT-NMR spectrometer, respectively. Chemical shifts were reported in parts per million (ppm) on the δ scale relative to the signal of TMS as an internal standard. Coupling constants (J) were given in hertz (Hz). All solution state ^{1}H NMR (300 MHz) experiments of **4** with different *n*-tetrabutylammonium salts were carried out in DMSO-d_6 at 25 °C. Mass spectra were obtained on a Water's Qtof Micro YA263 high resolution mass spectrometer in positive electron spray ionization mode for receptor, **L**, and negative electron spray ionization mode for complexes, **3**−**6**, in methanol solvent. Elemental analyses for the synthesized receptors and complexes were carried out with Perkin-Elmer 2500 series II elemental analyzer.

Synthesis of *N*, *N*′, *N*″-Tris[(2-amino-ethyl)-2,3,4,5,6-pentafluoro-benzylamine], L. The receptor **L** was synthesized as per our previously reported procedure.[27] Colorless single crystals suitable for X-ray diffraction analysis were obtained upon slow evaporation of methanolic solution of **L** after 5 days. Anal. Calcd for $C_{27}H_{21}F_{15}N_4$: C, 47.24; H, 3.08; N, 8.16. Found: C, 47.19; H, 3.12; N, 8.13. ^{1}H NMR (300 MHz, $CDCl_3$): δ 2.44 (m, 6H, NCH_2), 2.50 (m, 6H, NCH_2CH_2), 3.82 (s, 6H, $ArCH_2$), 1.60 (br, 3H, NH). ^{13}C NMR (75 MHz, $CDCl_3$): δ 40.63 (NCH_2), 46.61 (NCH_2CH_2), 54.25 ($ArCH_2$), 136.73, 138.59, 144.44, 146.42 (Ar). HRMS (+ESI): calcd; 686.4684, found; m/z 686.8922 $[LH]^+$.

Synthesis of $[H_3L(F)]\cdot[F]_2\cdot 2H_2O$, (3). To a 5 mL methanolic solution of **L** (0.069 g, 0.1 mmol), 3.1 equiv (0.081 g, 0.31 mmol) of tetrabutylammonium fluoride was added. After 2 h of continuous stirring at room temperature, the reaction mixture was filtered and allowed to evaporate slowly at room temperature. Colorless crystals of **3** suitable for single crystal X-ray studies were obtained after 4 days. Yield: 55%. Anal. Calcd for $C_{27}H_{28}F_{18}N_4O_2$: C, 41.44; H, 3.61; N, 7.16. Found: C, 41.32; H, 3.54; N, 7.11. ^{1}H NMR (300 MHz, DMSO-d_6): δ 2.61 (m, 6H, NCH_2CH_2), 3.14 (m, 6H, NCH_2CH_2), 4.22 (s, 6H, $ArCH_2$), 8.93 (br, 6H, NH_2^+). HRMS (-ESI): calcd; 705.4574, found; m/z 705.8087 $[L + F]^-$.

Synthesis of $[H_3L(OTs)]\cdot[OTs]_2$, (4). To the methanolic solution (5 mL) of **L** (0.69 g, 1 mmol) was added *p*-toluenesulphonic acid monohydrate (0.761 g, 4 mmol) as solid in one portion. The resulting clear solution was stirred at room temperature for 2 h. A 100 mL portion of cold diethyl ether was added to the reaction mixture with constant stirring for another 30 min. A white precipitate was formed. The precipitate was filtered off, washed several times with cold diethyl ether, and dried over anhydrous calcium chloride in a desiccator. Yield of **4** is 90%. Single crystals suitable for X-ray analysis were obtained by slow evaporation of methanolic solution of **4** at room temperature after complete evaporation of the solvent. Anal. Calcd for $C_{48}H_{45}F_{15}N_4O_9S_3$: C, 47.92; H, 3.77; N, 4.66. Found: C, 47.88; H, 3.80; N, 4.70; ^{1}H NMR (300 MHz, DMSO-d_6): δ 2.30 (s, 9H, Ts-CH_3), 2.84 (m, 6H,

dx.doi.org/10.1021/ic2011502 |*Inorg. Chem.* 2011, 50, 10693–10702

Table 1. Crystallographic Data and Refinement Details for L, Complexes 3−6

parameters	L	complex 3	complex 4	complex 5	complex 6
formula	$C_{27}H_{21}F_{15}N_4$	$C_{27}H_{24}F_{18}N_4O_2$	$C_{48}H_{45}F_{15}N_4O_9S_3$	$C_{41}H_{38}F_{15}N_5O_9S_2$	$C_{55}H_{52}F_{52}N_8O_2B_4Si$
M	686.48	778.50	1203.09	1093.88	1914.36
crystal habit	block	needle	block	block	block
crystal system	trigonal	monoclinic	monoclinic	triclinic	monoclinic
space group	$P\bar{3}$	$P2(1)/n$	$P2(1)/n$	$P\bar{1}$	$P2(1)/c$
a/Å	14.4998(12)	11.374(6)	8.3969(12)	8.132(3)	13.5797(17)
b/Å	14.4998(12)	15.129(8)	35.214(5)	15.167(6)	20.457(3)
c/Å	7.6888(15)	20.042(11)	17.523(3)	19.121(7)	27.338(3)
α/deg	90.00	90.00	90.00	85.038(5)	90.00
β/deg	90.00	103.529(14)	93.316(4)	88.786(6)	99.053(2)
γ/deg	120.00	90.00	90.00	84.381(6)	90.00
V/Å^3	1400.0(3)	3353.0(3)	5172.5(13)	2337.9(15)	7499.9(16)
Z	2	4	4	2	4
D_c/g cm^{-}3	1.629	1.542	1.545	1.554	1.695
μ/mm^{-1}	0.168	0.167	0.257	0.233	0.208
θ range	1.62°−27.02°	1.70°−19.23°	2.31°−18.59°	1.07°−16.13°	2.20°−20.56°
T/K	100(2)	100(2)	150(2)	100(2)	120(2)
F(000)	692	1568	2464	1116	3816
λ/Å	0.7107	0.7107	0.7107	0.7107	0.7107
total reflections	18942	17028	48400	8367	34468
unique reflections	2042	2789	9090	2333	12157
parameter used	167	461	715	651	1047
R1, $I > 2\sigma(I)$	0.0600	0.1175	0.0529	0.0393	0.0640
wR2, $I > 2\sigma(I)$	0.1628	0.3301	0.0976	0.0939	0.1584
goodness-of-fit	1.086	1.476	1.003	1.101	1.057

NCH_2CH_2), 3.21 (m, 6H, NCH_2CH_2), 4.34 (s, 6H, $ArCH_2$), 7.12 (d, 6H, Ts*H*, J = 7.5 Hz), 7.44 (d, 6H, Ts*H*, J = 7.5 Hz), 8.90 (br, 6H, NH_2^+). ^{13}C NMR (75 MHz, DMSO-d_6): δ 20.75 (Ts), 37.70 (NCH_2), 44.31 (NCH_2CH_2), 48.42 ($ArCH_2$), 106.11 (Ar), 125.31 (Ts), 128.13 (Ts), 138.23 (Ar), 144.55 (Ar). HRMS (-ESI): calcd; 1203.0628, found; m/z 1201.4169 $[H_2L + (TsO)_3]^-$, 1029.3391 $[HL + (TsO)_2]^-$, 857.2932 $[L + TsO]^-$.

Synthesis of $[H_3L(OTs)]\cdot[NO_3]\cdot[OTs]$, (5). Complex **4** (0.120 g, 0.10 mmol) was dissolved in methanol (5 mL), and 0.096 g (0.40 mmol) of tetrabutylammonium nitrate was added to the stirring solution. The resulting solution was stirred for 30 min at room temperature. The solution was filtered and allowed to evaporate at room temperature. Single crystals of **5** suitable for X-ray diffraction studies were obtained after 4 days. Yield of **5** is 45%. Anal. Calcd for $C_{41}H_{38}F_{15}N_5O_9S_2$: C, 45.02; H, 3.50; N, 6.40. Found: C, 45.08; H, 3.44; N, 6.36. ^{1}H NMR (300 MHz, DMSO-d_6): δ 2.29 (s, 9H, Ts-CH_3), 2.84 (m, 6H, NCH_2CH_2), 3.22 (m, 6H, NCH_2CH_2), 4.34 (s, 6H, $ArCH_2$), 7.12 (d, 6H, Ts*H*, J = 7.6 Hz), 7.44 (d, 6H, Ts*H*, J = 7.6 Hz), 8.89 (br, 6H, NH_2^+); HRMS(-ESI): calcd; 1093.8746, found; m/z 1091.6038 $[H_2L + (NO_3)^- + (TsO)_2]^-$, 1029.6498 $[HL + (TsO)_2]^-$, 857.5451 $[L + TsO]^-$, 748.4601 $[L + NO_3]^-$.

Synthesis of $[(H_3L)_2(SiF_6)]\cdot4[BF_4]\cdot CH_3OH\cdot H_2O$, (6). To a 5 mL methanolic solution of **L** (0.069 g, 1 mmol) was added 0.102 mL (3 mmol) of 48% tetrafluoroboric acid. The resulting solution was stirred for 2 h at room temperature and then it was kept for crystallization in a glass beaker. Colorless single crystals of **6** suitable for X-ray diffraction studies were isolated upon slow evaporation of the reaction mixture at 4 °C after 4 days. Yield of **5** is 45%. Anal. Calcd for $C_{55}H_{54}B_4F_{52}N_8O_2Si$: C, 34.44; H, 2.84; N, 5.84. Found: C, 34.46; H, 2.80; N, 5.84; ^{1}H NMR (300 MHz, DMSO-d_6): δ 2.69 (m, 6H, NCH_2), 3.16 (m, 6H, NCH_2CH_2), 4.13 (s, 6H, $ArCH_2$), 8.830 (br, 6H, NH_2^+). HRMS (-ESI): calcd; 1868.2590, found; m/z 862.1190 $[HL + BF_4]^-$.

X-ray Crystallographic Analyses. The crystallographic data, details of data collection, and refinement parameter for receptor, **L**, complexes **3**−**6** were summarized in Table 1. In each case, a single crystal of suitable size was selected from the mother liquor (except complex **4**) and immersed in paratone oil and then mounted on the tip of a glass fiber and cemented using epoxy resin. Intensity data for these crystals were collected using Mo K_α (λ = 0.7107 Å) radiation on a Bruker SMART APEX II diffractometer equipped with CCD area detector at 100 K for receptor, **L** and complexes **3** and **5**, 150 K for **4** and 120 K for complex **6**. Reflections were measured from a hemisphere of data collected with each frame covering 0.5° in ω. The data integration and reduction were processed with SAINT[41] software provided with the software package of SMART APEX II. An empirical absorption correction was applied to the collected reflections with SADABS.[42] The structures were solved by direct methods using SHELXTL[43] and were refined on F^2 by the full-matrix least-squares technique using the SHELXL-97[44] program package. Graphics were generated using PLATON[45] and MERCURY 2.3.[46] In all cases, the non-hydrogen atoms were refined anisotropically until the convergence. All the hydrogen atoms were geometrically positioned and treated as riding atoms. In complexes **3** and **6**, the hydrogen atoms of the lattice water molecules could not be located from the difference Fourier map.

Potentiometric Studies. All potentiometric[47−49] titration experiments were performed at 298 K, using carbonate-free NaOH with a Titrando model 809 along with a Metrohm combined glass electrode. The studies were performed in a solvent mixture of H_2O/MeOH (1:1 v/v) because of insolubility of the receptor in water. The protonation constants of the receptor, **L** were determined from titrations of a 1×10^{-3} M solution of **L** containing an excess of HNO_3 or TsOH (6×10^{-3} M) in the presence of $NaNO_3$ or NaOTs supporting electrolyte to maintain the total ionic strength of the solution at 0.1 M, respectively. Binding

dx.doi.org/10.1021/ic2011502 |*Inorg. Chem.* 2011, 50, 10693–10702

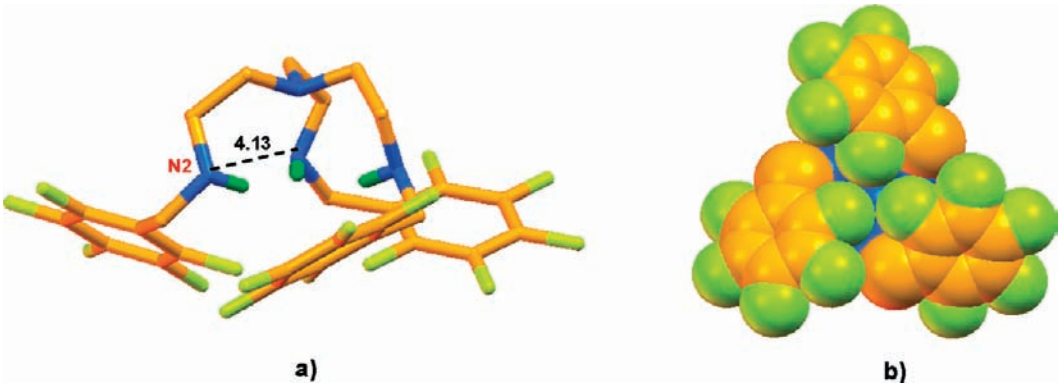

Figure 1. (a) Ball-stick and (b) spacefill model depicting the free receptor structure of **L** (contact distances are in Å, for clarity nonacidic hydrogen atoms are omitted).

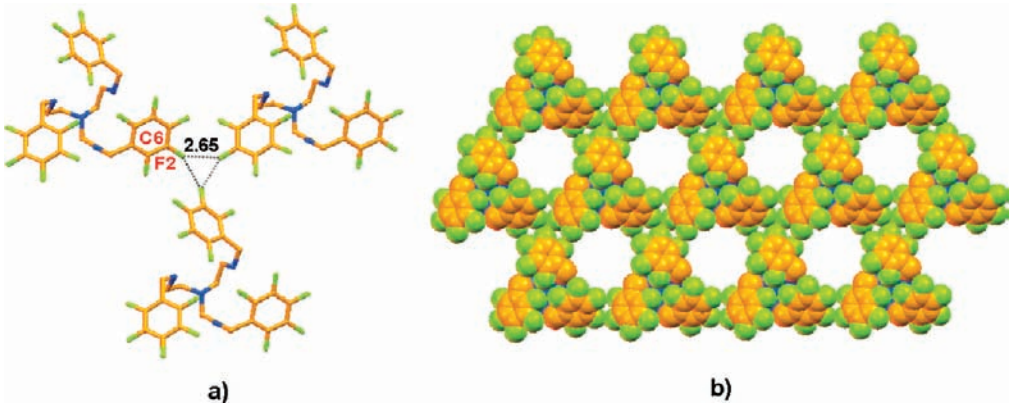

Figure 2. (a) Interactions in the crystal packing of **L**. (b) Spacefill model of 2D array of **L** along *b* axis (contact distances are in Å, for clarity hydrogen atoms are omitted).

constants of the receptor, **L** with different anions were determined from titrations of a 1×10^{-3} M receptor solution containing excess of HNO_3/TsOH (6×10^{-3} M) in the presence of 6×10^{-3} M of the corresponding NaX salt and supporting electrolyte $NaNO_3$/NaOTs to maintain the total ionic strength at 0.1 M. The range of accurate pH measurements was considered to be 2.6−10.0. Addition of sodium hydroxide beyond this pH region resulted in the precipitation of the receptor from the solution. Protonation constants and stability constants were calculated using the HYPERQUAD program.[50]

RESULTS AND DISCUSSION

The receptor **L** is synthesized as per our earlier report[27] in good yield and crystallized upon slow evaporation from the methanolic solution. We have attempted to isolate the protonated salt of **L** with anions of various geometries under different conditions. Here, we are able to isolate four new complexes $[H_3L(F)]\cdot[F]_2\cdot 2H_2O$ (**3**), $[H_3L(OTs)]\cdot[OTs]_2$ (**4**), $[H_3L(OTs)]\cdot[NO_3]\cdot[OTs]$ (**5**), and $[(H_3L)_2(SiF_6)]\cdot[BF_4]_4\cdot[CH_3OH]\cdot[H_2O]$ **6**, of **L** as crystals suitable for single crystal X-ray analyses other than previously reported chloride and bromide complexes **1** and **2**, respectively. All complexes are obtained in moderate yield. The detailed structural analyses of these complexes are described below.

Solid State Studies. *Crystallographic Description of* ***L***. The free receptor **L** crystallizes in a trigonal crystal system with $P\bar{3}$ space group. The molecule possesses a C_3 symmetry axis passing through the apical nitrogen N1. The average bond distance between the bridgehead nitrogen and the adjacent carbon is 1.478 Å. The ligand, **L**, possesses a preorganized perfect C_{3v} symmetric tripodal cleft (suitable for guest encapsulation within this cavity) with N···N distance of 4.133 Å where all three NH-protons are directed toward the cavity of the receptor (Figure 1a). The torsion angles involving $N1_{apical}CCN2_{amine}$ of each arm are in folded conformation with an angle of 65.82°, whereas torsion angles involving the carbon atoms connecting the terminal pentafluorophenyl rings in each arm are also in folded conformation with an angle of 58.92°.

The spacefill model of **L** (Figure 1b) depicts that the three pentafluorophenyl moieties are creating a surface of a positive quadrupole moment which can assist to attract the incoming oppositely charged anionic guest into the C_{3v} symmetric cleft of the receptor. The fluorine atom (F2) of a pentafluorophenyl ring is intermolecularly connected with two other pentafluorophenyl moieties of two neighboring ligands via a C−F···F−C interaction with a F···F distance of 2.65 Å, forming an equilateral triangular arrangement (Figure 2a). Crystal packing along *b* axis shows the formation of a honeycomb like cavity (Figure 2b), which could be due to the highly symmetrical arrangement of **L** in the solid state.

Crystallographic Description of Spherical Halide Complexes. The complex **3** crystallizes in a monoclinic crystal system with a $P2(1)/n$ space group. The asymmetric unit of complex **3**

dx.doi.org/10.1021/ic2011502 |*Inorg. Chem.* 2011, 50, 10693–10702

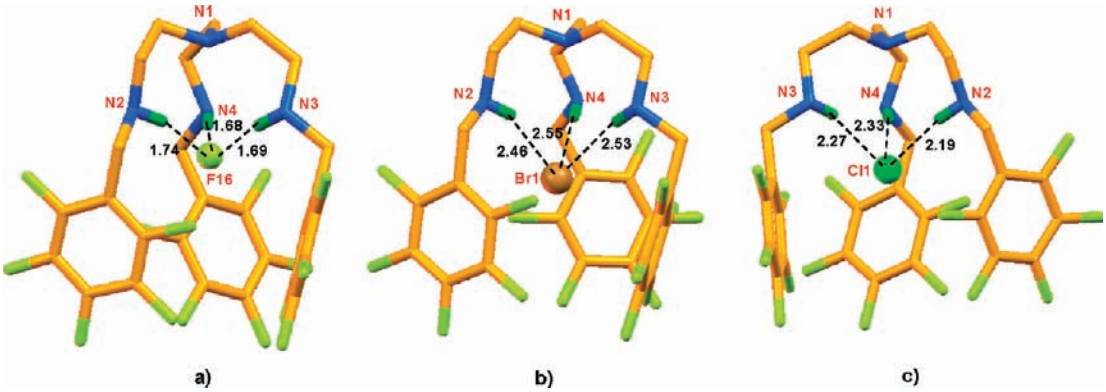

Figure 3. Ball-stick model of complexes **3**, **2**, and **1** depicting encapsulation of a fluoride (a), bromide (b), and chloride (c) anions in the cavity of $[H_3L]^{3+}$, respectively, where black dotted lines represent the $(N-H)^+\cdots X$ interactions (contact distances are in Å, for clarity nonacidic hydrogen atoms are omitted).

Table 2. Hydrogen Bonding Interactions of Encapsulated Fluoride with $[H_3L]^{3+}$ in Complex 3

D−H···A	H−A (Å)	D···A (Å)	∠D−H···A (deg)
N2−H2C···F16[a]	1.740	2.620(12)	166.3
N3−H3D···F16[a]	1.690	2.587(12)	173.8
N4−H4D···F16[a]	1.680	2.572(13)	171.9

[a] *x,y,z.*

contains one $[H_3L]^{3+}$ unit with an encapsulated fluoride ion, two water molecules as a solvent of crystallization, and two fluoride ions in the lattice. The fluoride encapsulated cleft possesses a distorted C_{3v} symmetric cavity which is evident from the slight difference in N···N distances (N2···N3 = 3.996 Å, N3···N4 = 4.045 Å, and N4···N2 = 3.981 Å, respectively) of basal plane. The average bond distance between the bridgehead nitrogen atom and the adjacent carbon atom in complex **3** is 1.463 Å which is close to the average N−C bridgehead bond distance in **L** (1.478 Å). It is also evident from the literature that when the bridgehead nitrogen in tren based systems is in the unprotonated state the average N−C distance ranges from 1.46 to 1.48 Å.[26,51−53] On the other hand, in the case of protonated bridgehead nitrogen the average N−C distance ranges from 1.50 to 1.51 Å.[51,52] This clearly indicates that the bridgehead nitrogen in **3** is in the unprotonated state and all the three secondary nitrogen atoms are in protonated form to satisfy the overall trinegative charge, though potentially four protonating sites are available in the receptor, **L**. The encapsulated fluoride in the cleft is held strongly via a $(N-H)^+\cdots F$ interaction with three ammonium moieties of $[H_3L]^{3+}$ unit (Figure 3a). The details of the hydrogen bonding interactions are listed in Table 2. The encapsulated fluoride ion is in distorted trigonal pyramidal geometry where it is located above the basal plane at a distance of 1.17 Å. The torsion angles involving $N1_{apical}CCN_{amine}$ are also in folded conformation similar to **L** with an angle of −63.86, −64.84, and −67.33° for three arms composed of the secondary amine nitrogen centers N2, N3, and N4, respectively, whereas the torsion angles involving the carbon atoms connecting the terminal pentafluorophenyl rings in each arm are in extended conformation with an angle ranging from 174.61 to 179°. The packing diagram of **3** viewed down the *a* axis is depicted in Figure 4, which shows a number of hydrogen bonding interactions of $[H_3L]^{3+}$ with the lattice fluoride ions F17 and F18 along

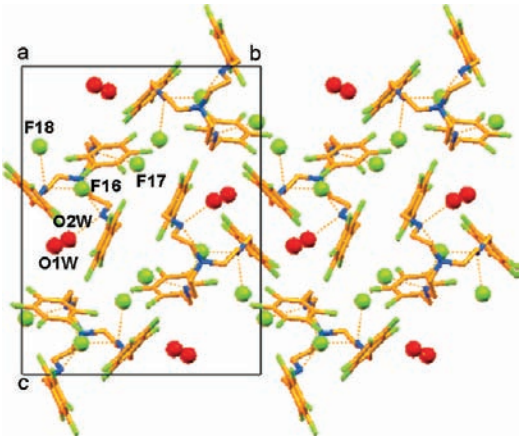

Figure 4. Packing diagram of $[H_3L(F)]\cdot[F]_2\cdot 2H_2O$, (**3**) as viewed down the *a* axis (for clarity hydrogen atoms are omitted).

Table 3. Hydrogen Bonding Interactions of Lattice Fluoride and Water with $[H_3L]^{3+}$ in Complex 3

D−H···A	D−H (Å)	H−A (Å)	D···A (Å)	∠D−H···A (deg)
N2−H2D···F18[a]	0.900	1.810	2.673(14)	159.9
N3−H3C···O2W[b]	0.900	1.770	2.649(16)	165.3
N4−H4C···F17[a]	0.900	1.840	2.716(15)	164.2
C3−H3A···O1W[a]	0.970	2.270	3.200(2)	160.0

[a] *x, y, z.* [b] *x, y, 1 + z.*

with two water molecules O1W and O2W. The lattice fluoride ions F17 and F18 are in strong $(N-H)^+\cdots F$ interactions with H4C and H2D of N4 and N2 atoms of the $[H_3L]^{3+}$, respectively. Further, the lattice water molecules O1W and O2W are involved in weak C−H···O and N−H···O hydrogen bonding interactions with the neighboring receptors. All the details of these hydrogen bonding interactions with symmetry code are tabulated in Table 3.

It is an interesting observation that the structural aspects of all the three halides (fluoride, bromide, and chloride) encapsulated complexes **3**, **2**, and **1** are iso-structural (Figure 3) in terms of hydrogen bonding patterns. The average bond distances between

the basal nitrogen atoms for complexes **3**, **2**, and **1** are 4.01, 4.36, and 4.26 Å, respectively, and all of them possess a distorted C_{3v} symmetric cavity. Thus, with the increase of anionic size from fluoride to bromide the modulation of N_4 cavity size of tren moiety takes place to engulf the incoming respective halide guests. Several attempts to encapsulate iodide in the cavity failed and always resulted in a semisolid mass. The distance between the basal plane containing nitrogen atoms and halides are 1.17 Å, 2.07 Å, and 1.89 Å respectively for complexes **3**, **2**, and **1**. Thus the comparative study on the location of halides in the $[H_3L]^{3+}$ cavity reveals that fluoride resides deep in the cavity among halides. In case of complex **3**, no short contact is observed between the encapsulated anionic guest fluoride and the positive charge cloud of the pentafluorophenyl rings as observed in complexes **1** and **2** (weak anion$\cdots\pi$ interactions). This could be due to the smallest size of fluoride guest, which is perfectly encapsulated deep in the N_4-cavity of **L** and satisfied by its tricoordination from three ammonium centers of the receptor unit.

Crystallographic Description of Tetrahedral Complexes. Complex $[H_3L(TsO)]\cdot[TsO]_2$, **4** crystallizes in a monoclinic crystal system with a space group $P2(1)/n$ as in the cases of complexes **1**−**3** whereas, complex $[H_3L(TsO)][(TsO)(NO_3)]$, **5**, crystallizes in a triclinic crystal system with a space group $P\bar{1}$. In complexes **4** and **5** the average bond distance between the bridgehead nitrogen and adjacent carbon is ∼1.47 Å which is also similar to that in free ligand, **L**, clearly indicates that the bridgehead nitrogen is in unprotonated state. In complex **4** the *p*-toluenesulphonate anion encapsulated cleft possesses a distorted C_{3v} symmetric cavity which is evident from the large difference in N$\cdots$N distances (N1$\cdots$N3 = 4.53 Å, N3$\cdots$N4 = 5.25 Å, and N4$\cdots$N1 = 5.84 Å, respectively) in the basal plane. The torsion angles of two arms involving $N2_{apical}CCN_{amine}$ are also in folded conformation similar to **L** with an angle of 63.80 and −51.77° for two arms composed of the secondary amine nitrogen centers N1 and N3, respectively, whereas the other arm has an extended conformation with a torsional angle of −164.94° involving the secondary nitrogen N4. The torsion angles involving the carbon atoms connecting the terminal pentafluorophenyl rings in each arm are in extended conformation with an angle ranging from 160.69 to 177.80°. Detailed structural analysis reveals that the asymmetric unit contains one $[H_3L]^{3+}$ unit and three *p*-toluenesulphonate anions. Among the three *p*-toluenesulphonate ions, one is encapsulated in the distorted C_{3v} symmetric tripodal cavity of $[H_3L]^{3+}$ whereas the other two are situated in the crystal lattice. The encapsulated *p*-toluenesulphonate is coordinated with the receptor $[H_3L]^{3+}$ via two strong $(N-H)^+\cdots O$ and four weak C−H$\cdots$O interactions as shown in the Figure 5a. In addition to the hydrogen bonding interactions in complex **4** there are two weak intermolecular $\pi\cdots\pi$ interactions between the electron deficient pentafluorophenyl ring of tripodal receptor and the electron rich phenyl ring of encapsulated and lattice *p*-toluenesulphonate (Figure 5b). The distance between the centroids of one of the lattice *p*-toluenesulphonate and the pentafluorophenyl ring of one arm of the receptor is 3.88 Å, whereas the $\pi\cdots\pi$ distance between the centroids of a encapsulated *p*-toluenesulphonate (from another complex in lattice) and pentafluorophenyl ring of other arm is 4.01 Å (Figure 5b). The details of the hydrogen bonding interactions with symmetry code of complex **4** are listed in Table 4.

Our attempt to replace the encapsulated *p*-toluenesulphonate by other oxo-anions like hydrogensulphate, dihydrogenphosphate, and perchlorate was unsuccessful. However, we were able to isolate the single crystals of complex $[H_3L(TsO)]$-$[(TsO)(NO_3)]$, **5**, upon addition of tetrabutylammonium nitrate to the complex **4**. Single crystal X-ray analysis of **5** shows that one of the lattice *p*-toluenesulphonate of **4** is exchanged by one nitrate, whereas encapsulated *p*-toluenesulphonate and the other lattice *p*-toluenesulphonate remain unchanged in the asymmetric unit as observed in **4**, though excess of nitrate salt is added during complexation (Figure 6a). Encapsulated *p*-toluenesulphonate in complex **5** shows similar hydrogen bonding patterns (Table 5) as observed in complex **4**. The planar lattice nitrate is sandwiched between two *p*-toluenesulphonate encapsulated tripodal units via $(N-H)^+\cdots O^-$ interactions

Table 4. Hydrogen Bonding Interactions of Encapsulated *p*-Toluenesulphonate with $[H_3L]^{3+}$ in 4

D−H$\cdots$A	H−A (Å)	D$\cdots$A (Å)	∠D−H$\cdots$A (deg)
N1−H1A$\cdots$O1[a]	2.10	2.991(4)	168
C20−H20A$\cdots$O2[a]	2.30	3.257(4)	167
C8−H8B$\cdots$O2[a]	2.50	3.208(4)	130
C20−H20A$\cdots$O3[a]	2.59	3.251(4)	126
N3−H3A$\cdots$O3[a]	1.98	2.849(4)	163
C21−H21A$\cdots$O3[a]	2.40	3.289(4)	152

[a] *x*, *y*, *z*.

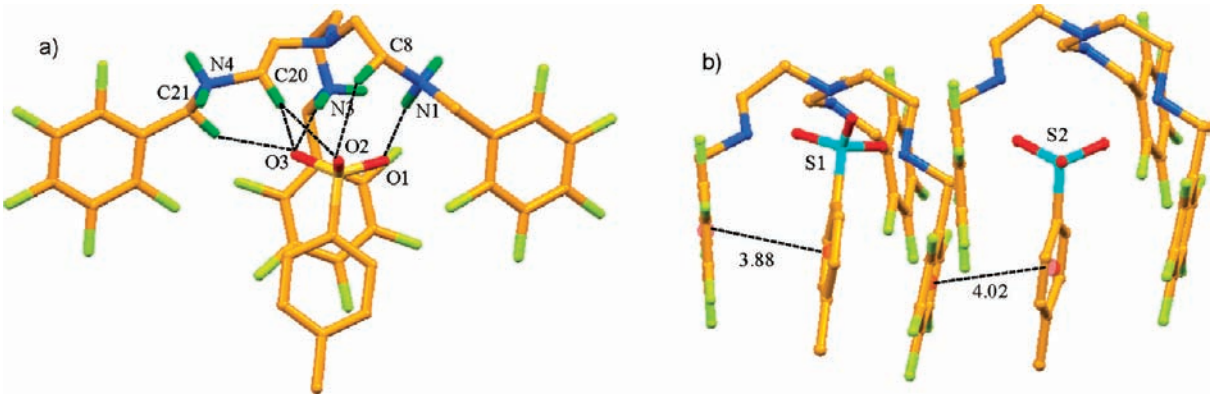

Figure 5. (a) Stick diagram depicting encapsulation of a *p*-toluenesulphonate inside the tripodal cavity, where dotted lines represent the $(N-H)^+\cdots O$ and C−H$\cdots$O interactions. (b) Possible $\pi\cdots\pi$ interactions between pentafluorophenyl ring and the phenyl ring of *p*-toluenesulphonate ion (contact distances are in Å, for clarity hydrogen atoms and other two counteranions are omitted).

dx.doi.org/10.1021/ic2011502 |*Inorg. Chem.* 2011, 50, 10693–10702

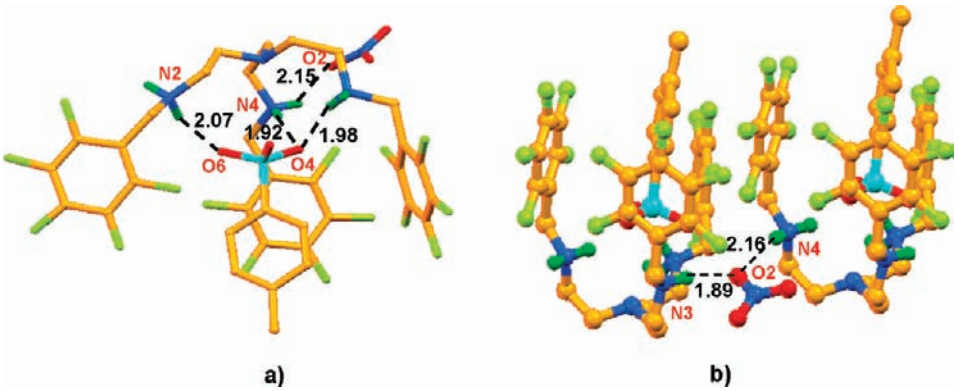

Figure 6. (a) Ball-stick diagram depicting encapsulation of a *p*-toluenesulphonate inside the tripodal cavity along with a nitrate ion in the lattice. (b) Binding model of the bridging lattice nitrate via $(N-H)^{+}\cdots O^{-}$ interactions (contact distances are in Å, hydrogens are omitted for clarity).

Table 5. Hydrogen Bonding Interactions of Encapsulated *p*-Toluenesulphonate with $[H_3L]^{3+}$ in 5

D−H···A	H−A (Å)	D···A (Å)	∠D−H···A (deg)
N2−H2D···O6[a]	2.070	2.920(9)	156.8
N3−H3C···O4[a]	1.990	2.862(9)	164.0
N4−H4C···O4[a]	1.920	2.781(9)	158.5

[a] *x, y, z.*

(Figure 6b). This result suggests that $[H_3L]^{3+}$ has higher affinity toward tetrahedral *p*-toluenesulphonate over planar nitrate ion.

Crystallographic Description of an Octahedral Complex, $[(H_3L)_2(SiF_6)]\cdot[BF_4]_4\cdot[CH_3OH][H_2O]$, **6**. The hexafluorosilicate complex of **L**, **6**, is obtained upon reaction of the methanolic solution of **L** with tetrafluoroboric acid. Complex $[(H_3L)_2(SiF_6)]\cdot[BF_4]_4\cdot[CH_3OH][H_2O]$, **6**, crystallizes in monoclinic crystal system with a space group $P2(1)/c$. The source of hexafluorosilicate in the system is presumably a result of glass corrosion in the experimental conditions. The asymmetric unit of **6** contains two $[H_3L]^{3+}$ units with one hexafluorosilicate, one methanol, and one water molecule as solvent of crystallization and the four noninteracting tetrafluoroborate anions. In complex **6**, the average bond distance between the bridgehead nitrogen and the adjacent carbon is ∼1.47 Å and indicates the bridgehead nitrogen is in unprotonated state as observed in cases of complexes **1**−**5**. Each of the two $[H_3L]^{3+}$ units (half capsules) of the hexafluorosilicate ion encapsulated capsule possesses a distorted C_{3v} symmetric cavity which is evident from the difference in N···N distances (one-half capsule: N2···N3 = 4.38 Å, N3···N4 = 4.27 Å, N4···N2 = 4.94 Å and other-half capsule: N6···N7 = 4.52 Å, N7···N8 = 4.39 Å, and N8···N6 = 4.90 Å, respectively) of basal planes. The torsion angles of the upper half capsule involving $N1_{apical}CCN_{amine}$ are in folded conformation with an angle of 86.99, 55.40, and 72.79° for the three arms composed of the secondary amine nitrogen centers N2, N3, and N4, respectively, whereas the torsion angles involving the carbon atoms connecting the terminal pentafluorophenyl rings in each arm are also in a folded conformation with angles of −17.47, −70.94, and −60.78°, respectively, as observed in **L**. Similarly, the torsion angles of the lower half capsule involving $N1_{apical}CCN_{amine}$ are also in folded conformation with angles of 95.46, 56.54, and 67.45° for the three arms composed of the secondary amine nitrogen centers N6, N7, and N8, respectively. The distance between two apical nitrogen atoms in the capsular assembly with an encapsulated octahedral hexafluorosilicate anion of **6** is 8.75 Å (Figure 7a). Figures 7b and 7c show that the octahedral hexafluorosilicate anion is completely buried deep inside the cavity of the dimeric capsule. The complexes of the triprotonated ligand, $[H_3L]^{3+}$, with spherical and tetrahedral anions, **1**−**5**, show monotopic encapsulation of the respective anionic guest. Interestingly, in complex **6** a hexafluorosilicate is encapsulated in a molecular capsule of two $[H_3L]^{3+}$ units which indeed supports that hexafluorosilicate plays a pivotal role in the assembly of two $[H_3L]^{3+}$ units to form a molecular capsule. The fluoride atoms (F31, F34, F35, and F36) of encapsulated hexafluorosilicate are involved in two hydrogen bonding interactions each via N−H···F contacts with two $[H_3L]^{3+}$ units. On the other hand, F32 is involved in three hydrogen bonding interactions via two C−H···F and one N−H···F contacts with the two $[H_3L]^{3+}$ units whereas F33 participates in one hydrogen bonding interaction, resulting in overall 12 hydrogen bonding interactions for encapsulated hexafluorosilicate with two $[H_3L]^{3+}$ units in the molecular capsule (Figure 8, Table 6).

Solution State Studies. *^{1}H NMR Studies.* The binding affinity of triprotonated tosylate complex of **L**, **4** toward different anions like fluoride, chloride, bromide, iodide, acetate, nitrate, and dihydrogenphosphate (as tetrabutylammonium salts) are examined by ^{1}H NMR studies in DMSO-d_6 at 298 K (Supporting Information, Figure S20 and S21). The addition of fluoride, acetate, and dihydrogenphosphate to the DMSO-d_6 solution of **4** shows disappearance of the $-NH_2^+$ resonance which could be due to the fast exchange of $-NH_2^+$ acidic protons in the NMR time scale in the presence of these more basic anions. Hence, NMR titrations with these anions could not be performed. A considerable downfield shift of $-NH_2^+$ resonances of **4** are observed upon addition of chloride ($\Delta\delta$ = 0.5 ppm) and bromide ($\Delta\delta$ = 0.1 ppm) anions under the same experimental conditions. The association constants of **4** with these two halides are reported in our earlier communication.[27] The addition of iodide, nitrate and hydrogensulphate anions to the DMSO-d_6 solution of **4** does not show any significant change in chemical shift of $-NH_2^+$ resonances indicating that these anions do not bind to the receptor.

Potentiometric Studies. The protonation constants of **L** and stability constants of $[H_3L]^{3+}$ with different anions in methanol/water (1:1 v/v) at 298 K are estimated by potentiometric

dx.doi.org/10.1021/ic2011502 |*Inorg. Chem.* 2011, 50, 10693–10702

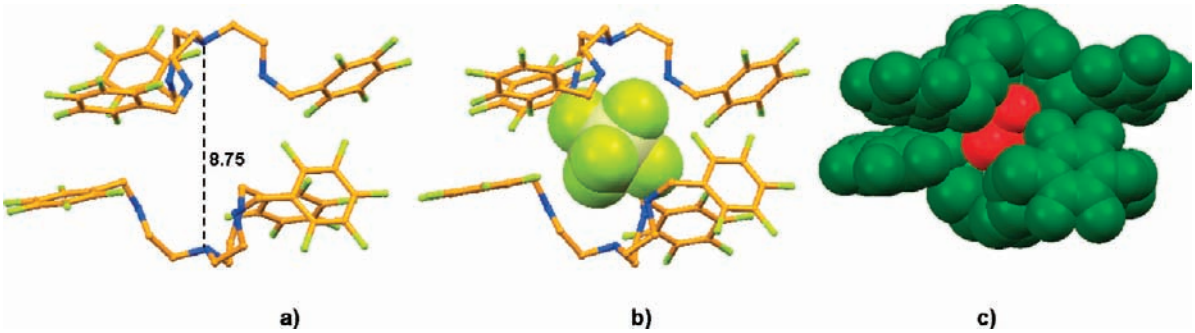

Figure 7. (a) Ball-stick model depicting the cavity size in between two half-capsule, (b) hexafluorosilicate anion assisted molecular capsular assembly formed by $[H_3L]^{3+}$, (c) spacefill model of the dimeric capsular assembly of complex **6** (contact distances are in Å, for clarity hydrogens and tetrafluoroborate counterion are omitted).

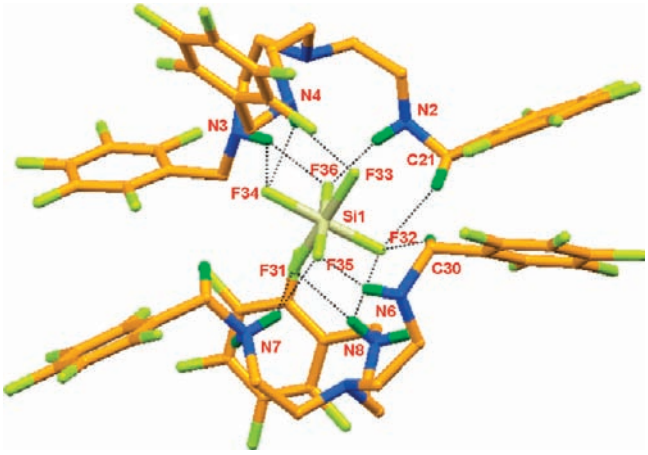

Figure 8. Ball-stick model showing the various hydrogen bonding interactions (dotted black lines) of the hexafluorosilicate from two surrounding $[H_3L]^{3+}$ units in complex **6** (for clarity hydrogens and tetrafluoroborate counterion are omitted).

Table 6. Hydrogen Bonding Interactions of Encapsulated Hexafluorosilicate with $[H_3L]^{3+}$ in 6

D−H···A	H−A (Å)	D···A (Å)	∠D−H···A (deg)
N7−H7B···F31[a]	2.140	2.726(4)	122.4
N8−H8B···F31[a]	2.150	3.035(4)	169.5
N8−H8B···F32[a]	2.290	2.845(4)	119.5
C21−H21B···F32[b]	2.340	3.250(6)	156.0
C30−H3A···F32[a]	2.350	3.187(5)	144.0
N4−H4B···F33[b]	2.080	2.813(4)	137.3
N4−H4B···F34[b]	2.230	2.988(5)	141.4
N3−H3A···F34[b]	2.250	2.818(4)	120.7
N6−H6B···F35[a]	1.920	2.747(4)	151.4
N7−H7B···F35[a]	1.990	2.790(4)	147.6
N2−H2B···F36[b]	1.780	2.662	164.9
N3−H3A···F36[b]	2.000	2.792(4)	146.5

[a] x, y, z . [b] $-x, y+1/2, -z+1/2$.

titration experiments. The protonation constants of **L** are determined in both $HNO_3/NaNO_3$ and TsOH/NaOTs medium. The protonation constants derived from these two experiments in different experimental conditions are comparable. Figure 9 shows the distribution diagram of mono, bis, and tris

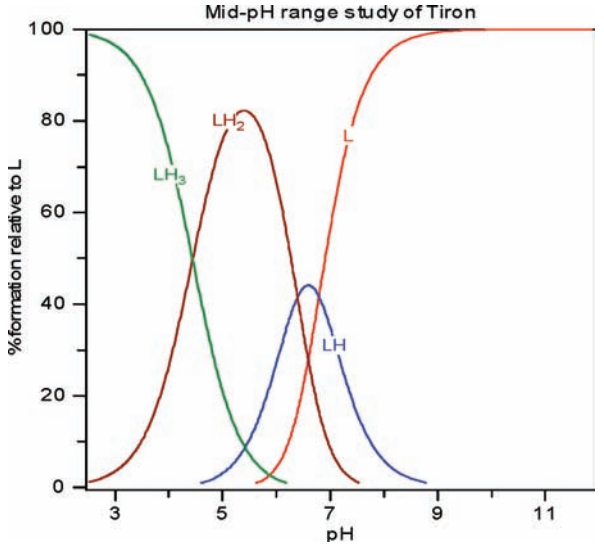

Figure 9. Species distribution diagram for the protonation of **L**. [**L**] = 1 mM, $[HNO_3]$ = 6 mM.

Table 7. Overall ($\log \beta_i^H$) and Stepwise Protonation ($\log K_i^H$) Constants of L in H_2O/MeOH (1:1 v/v)[a]

equilibrium reaction	$\log \beta_i^H$	equilibrium reaction	$\log K_i^H$
$L + H^+ = HL^+$	6.79	$L + H^+ = HL^+$	6.79
$L + 2H^+ = H_2L^{2+}$	13.18	$HL^+ + H^+ = H_2L^{2+}$	6.39
$L + 3H^+ = H_3L^{3+}$	17.62	$H_2L^{2+} + H^+ = H_3L^{3+}$	4.44

[a] T = 298.2 ± 0.1 K and I = 0.10 ± 0.01 M in $NaNO_3$.

protonated species of **L** in the pH region of 2.6−10.0. It is clear from the speciation diagram that the triprotonated species, $[H_3L]^{3+}$ predominates at pH values lower than 4.0. Upon gradual increment of pH of the solution, the triprotonated form in solution is steadily decreased with the formation of bisprotonated form, $[H_2L]^{2+}$. At around pH 5.5, the abundance of bisprotonated form of **L** is maximum along with simultaneous formation of monoprotonated species, $[HL]^+$. The maximum existence of monoprotonated species of **L** is around pH 7. The further increase in pH of the medium shows the existence of only free receptor, **L**, in unprotonated form as the dominating species. Three protonation constants are found for **L** corresponding to the successive protonation of three secondary amines, and they

dx.doi.org/10.1021/ic2011502 |*Inorg. Chem.* 2011, 50, 10693–10702

Table 8. Overall ($\log \beta_{HhLlAa}$) and Stepwise ($\log K_{HhLlAa}$) Association Constants[a] for the Indicated Equilibria in H_2O/MeOH (1: 1 v/v)[b]

equilibrium	F^-	Cl^-	Br^-	AcO^-	$H_2PO_4^-$	NO_3^-	SO_4^{2-}	TsO^-
$L + 3H^+ + A = H_3LA$	18.82[c]	18.30[c]	18.28[c]	19.07[c]	18.05[c]		18.30[c]	18.16[c]
	19.42[d]	18.9[d]	18.92[d]	19.02[d]	18.81[d]	18.82[d]		
$[H_3L]^{3+}+A = H_3LA$ (stepwise association constant)	1.2[c]	0.63[c]	0.66[c]	1.45[c]	0.43[c]		0.68[c]	0.54
	0.71[d]	0.19[d]	0.21[d]	0.31[d]	0.10[d]	0.11[d]		

[a] The association constants presented here represents the binding of **L** with different anions in triprotonated state whereas the binding affinity of **L** with these anions in diprotonated and monoprotonated states could not be determined accurately in these experimental conditions because of their weaker binding abilities in these states. [b] $T = 298.2 \pm 0.1$ K; $I = 0.10 \pm 0.01$ mol dm^{-3}, where, A = F^-, Cl^-, Br^-, AcO^-, $H_2PO_4^-$, NO_3^-, SO_4^{2-}, and TsO^-. Charges were omitted, for clarity, in species involving A. [c] In $NaNO_3$ supporting electrolyte. [d] In NaOTs supporting electrolyte.

are tabulated in Table 7. The stepwise protonation constants decrease steadily with the increase of degree of protonation of the receptor. This is due to the increase in the electrostatic repulsion between positive charges of the receptor. Although there are four basic nitrogen atoms in **L**, in the potentiometric study we could detect only the protonation of three nitrogen centers from the distribution diagram. It is indeed difficult to get the protonation constant value for the tetraprotonated form because at the higher pH region the ligand **L** is precipitated out from the solution. From the literature, it is evident that the potentiometric titration data on tripodal tetraamine ligands shows only three detectable protonation constants.[40,54−56]

The binding affinity of $[H_3L]^{3+}$ with different anions (fluoride, chloride, bromide, nitrate, dihydrogenphosphate, sulfate, and *p*-toluenesulphonate ion as their sodium salts) in MeOH/H_2O (1:1 v/v) solvent mixture is determined in the two different experimental conditions, 0.01 M HNO_3 (supporting electrolyte: $NaNO_3$, I = 0.1 M) and 0.01 M TsOH (supporting electrolyte: TsONa, I = 0.1 M). The association constants in these two different experimental conditions are tabulated in Table 8. It is clearly evident from the association constants that all anions have relatively lower binding affinity toward $[H_3L]^{3+}$ in methanol/water binary solvent system. Among all anions investigated, chloride, bromide, sulfate, dihydrogenphosphate, nitrate, and *p*-toluenesulphonate, bind to $[H_3L]^{3+}$ very weakly compared to fluoride and acetate anions which could be due to the increased basicity of these ions in this binary solvent system. From overall solution state studies, we found that there are some differences in the association constants evaluated by different techniques, that is, NMR titration (mentioned in our previous communication)[27] and potentiometric studies. This discrepancy may be attributed to the use of different solvent systems in NMR and potentiometric studies. In our earlier communication, NMR titration experiments are performed in polar aprotic DMSO-d_6 solvent whereas all potentiometric studies presented here have been carried out in a highly competing polar protic binary solvent mixture of MeOH/H_2O (1:1 v/v). Hence, the relatively lower association constants observed in the present investigation for chloride and bromide with $[H_3L]^{3+}$ could be due to hydration of these anions in the MeOH/H_2O solvent mixture whereas this effect is minimal when dimethylsulfoxide (DMSO) was used as a solvent of study in our earlier report.[27]

CONCLUSIONS

In conclusion, we have succeeded in encapsulating spherical (fluoride, chloride, and bromide) and tetrahedral (*p*-toluenesulphonate) anions in the C_{3v}-symmetric cavity of a pentafluorophenyl substituted tripodal amine receptor in triprotonated state. Although a phenyl substituted similar tripodal amine showed a preference toward bromide encapsulation in the C_{2v}-symmetric cleft of two arms of the triprotonated receptor.[26] Upon simple modification of substitutents in the tren-based tripodal amine receptor design, a marked difference in the anion recognition pattern is observed. Interestingly, this triprotonated amine can also act as a half capsule toward the formation of a molecular capsule assisted by octahedral hexafluorosilicate anion in the solid state. Further we have established the solution state anion binding pattern with triprotonated species of the ligand by potentiometric studies.

ASSOCIATED CONTENT

Supporting Information. Copies of ^{1}H NMR, ^{13}C NMR, and HRMS (ESI) spectra and CIF of receptor, **L** and complexes **3**−**6**. This material is available free of charge via the Internet at http://pubs.acs.org.

AUTHOR INFORMATION

Corresponding Author
*E-mail: icpg@iacs.res.in.

ACKNOWLEDGMENT

P.G. gratefully acknowledges the Department of Science and Technology (DST), New Delhi, India, for financial support. P.B. would like to acknowledge CSIR, New Delhi, India, for a Senior Research Fellowship. X-ray Crystallography study was performed at the DST-funded National Single Crystal X-ray Diffraction Facility at the Department of Inorganic Chemistry, IACS.

REFERENCES

(1) (a) *Supramolecular Chemistry of Anions*; Bianchi, A., Bowman-James, K., García-España, E., Eds.; Wiley-VCH: New York, 1997. (b) Beer, P. D.; Gale, P. A. *Angew. Chem., Int. Ed.* **2001**, *40*, 486–516. (c) Llinares, J. M.; Powell, D.; Bowman-James, K. *Coord. Chem. Rev.* **2003**, *240*, 57–75. (d) *The Encyclopedia of Supramolecular Chemistry*; Atwood, J. L., Steed, J. W., Eds.; Dekker: New York, 2004. (e) Bowman-James, K. *Acc. Chem. Res.* **2005**, *38*, 671–678. (f) García-España, E.; Díaz, P.; Llinares, J. M.; Bianchi, A. *Coord. Chem. Rev.* **2006**, *250*, 2952–2986. (g) Wichmann, K.; Antonioli, B.; Söhnel, T.; Wenzel, M.; Gloe, K.; Gloe, K.; Price, J. R.; Lindoy, L. F.; Blake, A. J.; Schröder, A. *Coord. Chem. Rev.* **2006**, *250*, 2987–3003. (h) Schottel, B. L.; Chifotides, H. T.; Dunbar, K. R. *Chem. Soc. Rev.* **2008**, *37*, 68–83.

(2) Zhu, S. S.; Staats, H.; Brandhorst, K.; Grunenberg, J.; Gruppi, F.; Dalcanale, E.; Lützen, A.; Rissanen, K.; Schalley, C. A. *Angew. Chem., Int. Ed.* **2008**, *47*, 788–792.

(3) Albrecht, M.; Wessel, C.; de Groot, M.; Rissanen, K.; Lüchow, A. *J. Am. Chem. Soc.* **2008**, *130*, 4600–4601.
(4) Li, Y.; Flood, A. H. *Angew. Chem., Int. Ed.* **2008**, *47*, 2649–2652.
(5) Götz, R. J.; Robertazzi, A.; Mutikainen, I.; Turpeinen, U.; Gamez, P.; Reedijk, J. *Chem. Commun.* **2008**, 3384–3386.
(6) Caltagirone, C.; Gale, P. A.; Hiscock, J. R.; Brooks, S. J.; Hursthouse, M. B.; Light, M. E. *Chem. Commun.* **2008**, 3007–3009.
(7) Bedford, R. B.; Betham, M.; Butts, C. P.; Coles, S. J.; Hursthouse, M. B.; Scully, P. N.; Tucker, J. H. R.; Wilkie, J.; Willener, Y. *Chem. Commun.* **2008**, 2429–2431.
(8) Turner, D. R.; Paterson, M. J.; Steed, J. W. *Chem. Commun.* **2008**, 1395–1397.
(9) Ng, K.-Y.; Felix, V.; Santos, S. M.; Rees, N. H.; Beer, P. D. *Chem. Commun.* **2008**, 1281–1283.
(10) Caltagirone, C.; Bates, G. W.; Gale, P. A.; Light, M. E. *Chem. Commun.* **2008**, 61–63.
(11) Schmuck, C.; Bickert, V. *J. Org. Chem.* **2007**, *72*, 6832–6839.
(12) Berryman, O. B.; Sather, B. P.; Hay, A. C.; Meisner, J. S.; Johnson, D. W. *J. Am. Chem. Soc.* **2008**, *130*, 10895–10897.
(13) Valiyaveettil, S.; Engbersen, J. F. J.; Verboom, W.; Reinhoudt, D. N. *Angew. Chem., Int. Ed. Engl.* **1992**, *32*, 900–901.
(14) Beer, P. D.; Chen, Z.; Goulden, A. J.; Graydon, A.; Stokes, S. E.; Wear, T. *J. Chem. Soc., Chem. Commun.* **1993**, 1834–1836.
(15) Beer, P. D.; Hopkins, P. K.; McKinney, J. D. *Chem. Commun.* **1999**, 1253–1254.
(16) Raposo, C.; Almaraz, M.; Martín, M.; Weinrich, V.; Mussóns, M. L.; Alcázar, V.; Caballero, M. C.; Morán, J. R. *Chem. Lett.* **1995**, 759–760.
(17) Danby, A.; Seib, L.; Bowman-James, K.; Alcock, N. W. *Chem. Commun.* **2000**, 973–974.
(18) Bazzicalupi, C.; Bencini, A.; Berni, E.; Bianchi, A.; Ciattini, S.; Giorgi, C.; Maoggi, S.; Paoletti, P.; Valtancoli, B. *J. Org. Chem.* **2002**, *67*, 9107–9110.
(19) Kavallieratos, K.; Danby, A.; Van Berkel, G. J.; Kelly, M. A.; Sachleben, R. A.; Moyer, B. A.; Bowman-James, K. *Anal. Chem.* **2000**, *72*, 5258–5264.
(20) Lakshminarayanan, P. S.; Suresh, E.; Ghosh, P. *Inorg. Chem.* **2006**, *45*, 4372–4380.
(21) Custelcean, R. B.; Moyer, A.; Hay, B. P. *Chem. Commun.* **2005**, 5971–5973.
(22) Jose, D. A.; Kumar, D. K.; Ganguly, B.; Das, A. *Inorg. Chem.* **2007**, *46*, 5817–5819.
(23) Custelcean, R.; Remy, P.; Bonnesen, P. V.; Jiang, De-en.; Moyer, B. A. *Angew. Chem., Int. Ed.* **2008**, *47*, 1866–1870.
(24) Wu, B.; Liang, J.; Yang, J.; Jia, C.; Yang, X.-J.; Zhang, H.; Tang, N.; Janiak, C. *Chem. Commun.* **2008**, 1762–1764.
(25) Bryantsev, V. S.; Hay, B. P. *Org. Lett.* **2005**, *7*, 5031–5034.
(26) Hossain, M. A.; Liljegren, J. A.; Powell, D.; Bowman-James, K. *Inorg. Chem.* **2004**, *43*, 3751–3755.
(27) Lakshminarayanan, P. S.; Ravikumar, I.; Suresh, E.; Ghosh, P. *Inorg. Chem.* **2007**, *46*, 4769–4771.
(28) Lakshminarayanan, P. S.; Ravikumar, I.; Suresh, E.; Ghosh, P. *Chem. Commun.* **2007**, 5214–5216.
(29) Jia, C.; Wu, B.; Li, S.; Huang, X.; Zhao, Q.; Li, Q.-S.; Yang, X.-J. *Angew. Chem., Int. Ed. Engl.* **2011**, *50*, 486–490.
(30) Ravikumar, I.; Lakshminarayanan, P. S.; Arunachalam, M.; Suresh, E.; Ghosh, P. *Dalton Trans.* **2009**, 4160–4168.
(31) Custelcean, R.; Bock, A.; Moyer, B. A. *J. Am. Chem. Soc.* **2010**, *132*, 7177–7185.
(32) Tobey, S. L.; Jones, B. D.; Anslyn, E. V. *J. Am. Chem. Soc.* **2003**, *125*, 4026–4027.
(33) Işıklan, M.; Saeed, M. A.; Pramanik, A.; Wong, B. M.; Fronczek, F. R.; Hossain, M. A. *Cryst. Growth Des.* **2011**, *11*, 959–963.
(34) Motekaitis, R. J.; Martell, A. E.; Murase, I.; Lehn, J.-M.; Hosseini, M. W. *Inorg. Chem.* **1988**, *27*, 3630–3636.
(35) Mason, S.; Llinares, J. M.; Morton, M.; Clifford, T.; Bowman-James, K. *J. Am. Chem. Soc.* **2000**, *122*, 1814–1815.
(36) Aguilar, J. A.; Clifford, T.; Danby, A.; Llinares, J. M.; Mason, S.; García-España, E.; Bowman-James, K. *Supramol. Chem.* **2001**, *13*, 405–417.
(37) Hossain, M. A.; Llinares, J. M.; Mason, S.; Morehouse, P.; Powell, D.; Bowman-James, K. *Angew. Chem., Int. Ed.* **2002**, *41*, 2335–2338.
(38) Hossain, M. A.; Morehouse, P.; Powell, D.; Bowman-James, K. *Inorg. Chem.* **2005**, *44*, 2143–2149.
(39) Hazell, R. G.; Rasmussen, S. E. *Acta Chem. Scand.* **1968**, *22*, 348–350.
(40) Bazzicalupi, C.; Bencini, A.; Bianchi, A.; Danesi, A.; Giorgi, C.; Valtancoli, B. *Inorg. Chem.* **2009**, *48*, 2391–2398.
(41) Sheldrick, G. M. *SAINT and XPREP*, 5.1 ed.; Siemens Industrial Automation Inc.: Madison, WI, 1995. .
(42) *SADABS, empirical absorption Correction Program*; University of Göttingen: Göttingen, Germany, 1997.
(43) Sheldrick, G. M. *SHELXTL Reference Manual*, Version 5.1; Bruker AXS: Madison, WI, 1997.
(44) Sheldrick, G. M. *SHELXL-97, Program for Crystal Structure Refinement*: University of Göttingen: Göttingen, Germany, 1997.
(45) Spek, A. L. *PLATON-97*; University of Utrecht: Utrecht, The Netherlands, 1997.
(46) *Mercury 2.2*, Supplied with Cambridge Structural Database; CCDC: Cambridge, U.K, 2003−2004.
(47) Mateusa, P.; Berniera, N.; Delgado, R. *Coord. Chem. Rev.* **2010**, *254*, 1726–1746.
(48) Mateus, P.; Delgado, R.; Brandão, P.; Carvalho, S.; Félix, V. *Org. Biomol. Chem.* **2009**, *7*, 4661–4673.
(49) Mateus, P.; Delgado, R.; Brandão, P.; Félix, V. *J. Org. Chem.* **2009**, *74*, 8638–8646.
(50) Gans, P.; Sabatini, A.; Vacca, A. *Talanta* **1996**, *43*, 1739–1753.
(51) Danby, A.; Seib, L.; Alcock, N. A.; Bowman-James, K. *Chem. Commun.* **2000**, 973–974.
(52) Lakshminarayanan, P. S.; Suresh, E.; Ghosh, P. *Inorg. Chem.* **2006**, *45*, 4372–4380.
(53) Lakshminarayanan, P. S.; Ravikumar, I.; Suresh, E.; Ghosh, P. *Cryst. Growth Des.* **2008**, *8*, 2842–2852.
(54) Thaler, F.; Hubbard, C. D.; Heinemann, F. W.; van Eldik, R.; Schindler, S.; Fábián, I.; Dittler-Klingemann, A. M.; Hahn, F. E.; Orvig, C. *Inorg. Chem.* **1998**, *37*, 4022–4029.
(55) Fischmann, A. J.; Warden, A. C.; Black, J.; Spiccia, L. *Inorg. Chem.* **2004**, *43*, 6568–6578.
(56) Menif, R.; Reibenspies, J.; Martell, A. E. *Inorg. Chem.* **1991**, *30*, 3446–3454.